Transient conjugated heat transfer in microchannels: Integral transforms with single domain formulation

CrossMark

Diego C. Knupp [a], Renato M. Cotta [b,*], Carolina P. Naveira-Cotta [b], Sadik Kakaç [c]

[a] Instituto Politécnico, Universidade do Estado do Rio de Janeiro, IPRJ/UERJ, Laboratory of Experimentation and Numerical Simulation in Heat and Mass Transfer, LEMA, Dept. of Mechanical Engineering and Energy, Nova Friburgo, RJ, Brazil
[b] Universidade Federal do Rio de Janeiro — COPPE & POLI, UFRJ, Laboratory of Transmission and Technology of Heat, Laboratory of Microfluidics and Micro-systems, Mechanical Engineering Department, Cx. Postal 68503, Rio de Janeiro, RJ 21945-970, Brazil
[c] TOBB University of Economics & Technology, Ankara, Turkey

A B S T R A C T

The transient behaviour of conjugated heat transfer in laminar microchannel flow is investigated, taking into account the axial diffusion effects, which are often of relevance in microchannels, and including pre-heating or pre-cooling of the region upstream of the heat exchange section. The solution methodology is based on the Generalized Integral Transform Technique (GITT), as applied to a single domain formulation proposed for modelling the heat transfer phenomena at both the fluid stream and the channel wall regions. By making use of coefficients represented as space dependent functions with abrupt transitions occurring at the fluid—wall interfaces, the mathematical model carries the information concerning the transition of the two domains, unifying the model into a single domain formulation with variable co-efficients. The proposed approach is illustrated for microchannels with polymeric walls of different thicknesses. The accuracy of approximate internal wall temperature estimates deduced from measure-ments of the external wall temperatures, accounting only for the thermal resistance across the wall thickness, is also analyzed.

© 2014 Elsevier Masson SAS. All rights reserved.

1. Introduction

Transient forced convection in channels has been a subject of intense research activity since the earlier works of S. Kakaç and collaborators [1–3], in the context of fundamental work aimed at the development of analytical solution techniques and the experi-mental validation of proposed models and methodologies, for both the fully transient and periodic states, in either laminar or turbulent regimen [4–16]. This research front was later on further pursued in the direction of extending the previously developed hybrid tools to handle both transient flow and transient convection problems in microchannels within the slip flow regime [17–22].

Most of these works on transient forced convection were based on extension or application of the ideas in the Generalized Integral Transform Technique (GITT), a well-established hybrid numerical-analytical solution methodology for convection-diffusion problems [23–28]. Also, most of the works cited above do not account for wall conjugation effects or at most

consider only the influence of the wall thermal capacitance on the transient behavior of the fluid temperature evolution along the channel [7–9]. A few works have analyzed the effects of heat conduction along the wall, in addition to thermal capacitance, in the transient behavior of internal forced convection with wall participation [29–35].

Although transients might be very rapid during convective heat transfer within microchannels, due to the short length and time scales involved, conjugation effects might play a major role in the transient behavior of thermal microsystems, considerably increasing the duration of the thermal responses to different timewise disturbances. Conjugated heat transfer is in fact a typical example of an effect that may have significant importance in micro-scale convective heat transfer but is often neglected in macro-scale situations. Nunes et al. [36] presented a theoretical-experimental study of steady state conjugated heat transfer in microchannels, with the theoretical model taking into account heat conduction along the microchannel walls length, extending the work devel-oped in Ref. [37]. This work is also based on the Generalized Integral Transform Technique, modeled through a mixed lumped-differential thermal formulation which proposes lumping over the wall transversal direction only and accounting for the longi-tudinal heat conduction. The approach in Ref. [36] yields simulation

* Corresponding author.
   E-mail addresses: renatocotta@hotmail.com, cotta@mecanica.coppe.ufrj.br (R. M. Cotta).

Nomenclature

Bi	Biot number
D_h	hydraulic diameter
g_i	source term in the transformed problem, Eq. (16a)
h_e	heat transfer coefficient at the channel external wall
K	dimensionless thermal conductivity
k	thermal conductivity
L	thickness of the channel wall
L_e	distance from the channel centerline to the external face of the channel wall
L_f	channel height
L_w	channel width
M	truncation order of the auxiliary problem
N_ζ, N_ξ, N_Ω, N_ϕ	Normalization integrals corresponding to the eigenfunctions ζ, ξ, Ω and ϕ
N	truncation order of the temperature field expansions
Pe	Péclet number
T	temperature field
t	time variable
U	dimensionless fully developed velocity profile
u	velocity profile
W	dimensionless heat capacity
w	heat capacity
Y	dimensionless transversal coordinate
y	transversal coordinate
Z	dimensionless longitudinal coordinate
z	longitudinal coordinate

Greek letters

α	thermal diffusivity, Eq. (2)
$\beta,\alpha,\lambda,\upsilon,\mu$	eigenvalues corresponding to ξ,ζ,Ω, ϕ, and ψ respectively
δ	transition function
ζ	eigenfunction of the insulated region eigenvalue problem
η	parameter that controls the transition spatial behavior
θ	dimensionless temperature field
ν	kinematic viscosity
ξ	eigenfunction of the heat exchange section eigenvalue problem
τ	dimensionless time
ϕ	eigenfunction of the auxiliary problem corresponding to insulated region eigenvalue problem
ψ	eigenfunction
Ω	eigenfunction of the auxiliary problem corresponding to the heat exchange section eigenvalue problem

Subscripts & superscripts

ad	quantity corresponding to the insulated upstream region
i,m,n	order of eigenquantities
—	integral transform
~	normalized eigenfunction
f	fluid
s	solid
in	channel inlet
∞	external environment

results in much better agreement with the available experimental data obtained in the same work, reconfirming the importance of wall conjugation in micro-channels applications.

More recently, the reformulation of conjugated conduction-convection problems has been proposed as a single region model that fully accounts for the local heat transfer at both the fluid flow and the channel wall regions [38–40]. This novel approach allows for a straightforward hybrid analytical-numerical analysis of more involved conjugated heat transfer problem formulations, again based on the GITT in either total or partial transformation schemes. By introducing coefficients represented as space variable functions with abrupt transitions occurring at the fluid—wall interfaces, the mathematical model carries the information concerning the two original domains of the problem.

In the present work, making use of this single domain formulation and the integral transform method, the transient behavior of conjugated heat transfer in laminar microchannel flow is investigated, taking into account the thermal capacitance and transversal and axial diffusion effects at both the fluid and the walls, and including the participation of the wall and fluid regions upstream of the heat exchange section. For illustration purposes, an existing experimental configuration is considered, consisting of a rectangular microchannel etched on a polyester resin substrate [41], with different wall thicknesses. We also verify the accuracy and merits of a simple thermal resistance model, applied across the wall thickness, in estimating the internal wall temperatures from available measurements of the external wall temperatures.

2. Problem formulation and solution methodology

Fig. 1 depicts a schematic representation of the problem under consideration. The channel wall is considered to participate in the heat transfer problem through both transversal and longitudinal heat conduction. We consider a laminar incompressible internal flow of a Newtonian fluid inside a rectangular channel with height and width given by L_f and L_w, respectively, being $L_w \gg L_f$ so that it can be represented by a flow between parallel plates, undergoing conjugated heat transfer between the fluid and bounding walls. The external face of the microchannel exchanges heat with the surrounding environment by means of convection with a known heat transfer coefficient, h_e. It is also considered that the microchannel heat exchange section, $0 \leq z \leq z_\infty$, may exchange heat with the transversally insulated upstream region, $-z_{ad,\infty} \leq z \leq 0$. The fluid flows with a fully developed velocity profile $u_f(y)$, and with uniform inlet temperature, T_{in}. The flow is assumed to be hydrodynamically
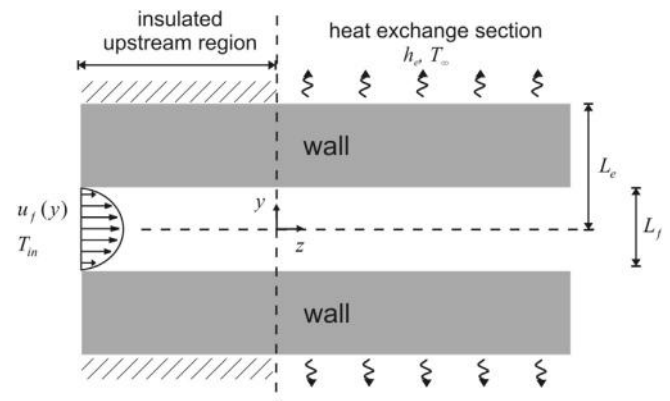

Fig. 1. Schematic representation of the transient conjugated heat transfer problem in a microchannel with upstream region participation.

developed but thermally developing, with negligible viscous dissipation and temperature independent physical properties.

Defining space variable coefficients with abrupt transitions, the dimensionless formulation of the conjugated problem as a single domain model is given by Ref. [40]:

$$W(Y)\frac{\partial\theta(Y,Z,\tau)}{\partial\tau} + U(Y)W(Y)\frac{\partial\theta}{\partial Z} = \frac{K(Y)}{Pe^2}\frac{\partial^2\theta}{\partial Z^2} + \frac{4}{\sigma^2}\frac{\partial}{\partial Y}\left(K(Y)\frac{\partial\theta}{\partial Y}\right),$$
$$0 < Y < 1, \quad -Z_{ad,\infty} < Z < Z_\infty, \quad \tau > 0$$
(1a)

$$\frac{\partial\theta}{\partial Y}\bigg|_{Y=0} = 0, \quad \frac{\partial\theta}{\partial Y}\bigg|_{Y=1} + Bi_{ef}(Z)\theta(Y=1,Z,\tau) = 0,$$
$$-Z_{ad,\infty} < Z < Z_\infty, \quad \tau > 0$$
(1b,c)

$$\theta(Y,Z=-Z_{ad,\infty},\tau) = 1, \quad \frac{\partial\theta}{\partial Z}\bigg|_{Z=Z_\infty} = 0, \quad 0 < Y < 1, \quad \tau > 0 \quad (1d,e)$$

$$\theta(Y,Z,\tau=0) = 0, \quad 0 < Y < 1, \quad -Z_{ad,\infty} < Z < Z_\infty \quad (1f)$$

with:

$$U(Y) = \begin{cases} U_f(Y), & \text{if } 0 < Y < Y_i \\ 0, & \text{if } Y_i < Y < 1 \end{cases} \quad K(Y) = \begin{cases} 1, & \text{if } 0 < Y < Y_i \\ k_s/k_f, & \text{if } Y_i < Y < 1 \end{cases}$$
$$W(Y) = \begin{cases} 1, & \text{if } 0 < Y < Y_i \\ w_s/w_f, & \text{if } Y_i < Y < 1 \end{cases}$$
(1g –i)

$$Bi_{ef}(Z) = \begin{cases} 0, & \text{if } -Z_{ad,\infty} < Z < 0 \\ Bi, & \text{if } 0 < Z < Z_\infty \end{cases} \quad (1j)$$

where the following dimensionless groups have been employed:

$$Z = \frac{z/D_h}{RePr} = \frac{z}{D_h Pe}; \quad Y = \frac{y}{L_e}; \quad U = \frac{u}{u_{av}}; \quad \theta = \frac{T - T_\infty}{T_{in} - T_\infty};$$
$$K = \frac{k}{k_f}; \quad Re = \frac{u_{av}D_h}{\nu}; \quad Pr = \frac{\nu}{\alpha}; \quad Pe = RePr = \frac{u_{av}D_h}{\alpha};$$
$$\alpha = \frac{k_f}{w_f}; \quad Bi = \frac{h_e L_e}{k_s}; \quad \sigma = \frac{L_e}{L_f}; \quad \tau = \frac{\alpha t}{D_h^2}; W = \frac{w}{w_f}; \quad Y_i = \frac{L_f}{2L_e}$$
(2)

and where y and z are the transversal and longitudinal variables, respectively, t is the time variable, u is the fully developed velocity profile, T is the temperature field, k and w are the thermal conductivity and heat capacity, respectively, ν is the kinematic viscosity and the hydraulic diameter is given by $D_h = 2L_f$. The subscripts s and f indicate the solid (channel wall) and fluid stream regions, respectively. In order to solve through integral transformation the problem given by Eq. (1), we define the following integral transform pair:

$$\text{transform}: \bar{\theta}_i(Z,\tau) = \int_0^1 W(Y)\tilde{\psi}_i(Y,Z)\theta(Y,Z,\tau)dY \quad (3a)$$

$$\text{inverse}: \theta(Y,Z,\tau) = \sum_{i=1}^\infty \tilde{\psi}_i(Y,Z)\bar{\theta}_i(Z,\tau) \quad (3b)$$

where the normalized eigenfunctions $\tilde{\psi}_i(Y,Z)$ and associated eigenvalues $\mu_i(Z)$ are represented, respectively, by $\tilde{\zeta}_i(Y)$ and α_i,

for $-Z_{ad,\infty} < Z < 0$, and by $\tilde{\tilde{\xi}}_i(Y)$ and β_i, for $0 < Z < Z_\infty$. Thus, it is convenient to represent as a single continuous function the transition between the upstream and heat exchange regions in the form:

$$\tilde{\psi}_i(Y,Z) = \tilde{\tilde{\xi}}_i(Y) + \left[\tilde{\zeta}_i(Y) - \tilde{\tilde{\xi}}_i(Y)\right]\delta(Z), \text{ and}$$
$$\mu_i(Z) = \beta_i + (\alpha_i - \beta_i)\delta(Z)$$
(4a,b)

where the transition function may be taken as

$$\delta(Z) = \frac{1}{1 + \exp(\eta Z)} \quad (4c)$$

where the parameter η controls the spatial transition behavior and thus may be adequately chosen in order to make the transition as abrupt as necessary.

The normalized eigenfunctions $\tilde{\tilde{\xi}}_i(Y)$ and associated eigenvalues β_i come from the following eigenvalue problem, corresponding to the heat exchange section:

$$\frac{4}{\sigma^2}\frac{d}{dY}\left(K(Y)\frac{d\xi(Y)}{dY}\right) + W(Y)\beta^2\xi(Y) = 0 \quad (5a)$$

$$\frac{d\xi}{dY}\bigg|_{Y=0} = 0, \quad \frac{d\xi}{dY}\bigg|_{Y=1} + Bi\xi(Y=1) = 0 \quad (5b,c)$$

whereas the normalized eigenfunctions $\tilde{\zeta}_i(Y)$ and associated eigenvalues α_i, corresponding to the upstream region, come from:

$$\frac{4}{\sigma^2}\frac{d}{dY}\left(K(Y)\frac{d\zeta(Y)}{dY}\right) + W(Y)\alpha^2\zeta(Y) = 0 \quad (6a)$$

$$\frac{d\zeta}{dY}\bigg|_{Y=0} = 0, \quad \frac{d\zeta}{dY}\bigg|_{Y=1} = 0 = 0 \quad (6b,c)$$

and the normalized eigenfunctions are calculated as:

$$\tilde{\xi}_i(Y) = \frac{\xi_i(Y)}{\sqrt{N_{\xi_i}}}, \text{ and } \tilde{\zeta}_i(Y) = \frac{\zeta_i(Y)}{\sqrt{N_{\zeta_i}}} \quad (7a,b)$$

with the normalization integrals given by:

$$N_{\xi_i} = \int_0^1 W(Y)\xi_i^2(Y)dY, \text{ and } N_{\zeta_i} = \int_0^1 W(Y)\zeta_i^2(Y)dY \quad (8a,b)$$

The eigenvalue problems defined in Eqs. (5) and (6) can be handled by the GITT itself with the proposition of a simpler auxiliary problem and expanding the unknown eigenfunctions in terms of the chosen basis [42,43].

Here, the simplest possible auxiliary problems have been chosen, keeping the boundary conditions of the original problem, which for the heat exchange section is written as:

$$\frac{d^2\Omega_n(Y)}{dY^2} + \lambda_n^2\Omega_n(Y) = 0 \quad (9a)$$

$$\frac{d\Omega_n(Y)}{dY}\bigg|_{Y=0} = 0, \quad \frac{d\Omega_n}{dY}\bigg|_{Y=1} + Bi\,\Omega_n(Y=1) = 0 \quad (9b,c)$$

and for the upstream region is written as:

$$\frac{d^2\phi_n(Y)}{dY^2} + v_n^2\phi_n(Y) = 0 \tag{10a}$$

$$\left.\frac{d\phi_n(Y)}{dY}\right|_{Y=0} = 0, \quad \left.\frac{d\phi_n(Y)}{dY}\right|_{Y=1} = 0 \tag{10b,c}$$

The proposed expansions of the original eigenfunctions are then given by:

$$\xi_i(Y) = \sum_{n=1}^{\infty} \tilde{\Omega}_n(Y)\overline{\xi}_{i,n}, \quad \text{inverse} \tag{11a}$$

$$\overline{\xi}_{i,n} = \int_0^1 \xi_i(Y)\tilde{\Omega}_n(Y)dY, \quad \text{transform} \tag{11b}$$

and

$$\zeta_i(Y) = \sum_{n=0}^{\infty} \tilde{\phi}_n(Y)\overline{\zeta}_{i,n}, \quad \text{inverse} \tag{12a}$$

$$\overline{\zeta}_{i,n} = \int_0^1 \zeta_i(Y)\tilde{\phi}_n(Y)dY, \quad \text{transform} \tag{12b}$$

where the normalized eigenfunctions $\tilde{\Omega}_n(Y)$ and $\tilde{\phi}_n(Y)$ are given by the following expressions:

$$\tilde{\Omega}_n(Y) = \frac{\Omega_n(Y)}{\sqrt{N_{\Omega_n}}}, \text{ and } \tilde{\phi}_n(Y) = \frac{\phi_n(Y)}{\sqrt{N_{\phi_n}}} \tag{13a,b}$$

with the normalization integrals given by:

$$N_{\Omega_n} = \int_0^1 \Omega_n^2 dY, \text{ and } N_{\phi_n} = \int_0^1 \phi_n^2 dY \tag{13c,d}$$

The integral transformation of the eigenvalue problems with space variable coefficients, given by the problems defined in Eqs. (5) and (6), is then performed by operating on Eq. (5a) with $\int_0^1 \tilde{\Omega}_n(Y) - dY$ and on Eq. (6a) with $\int_0^1 \tilde{\phi}_n(Y) - dY$, respectively. For the problem defined in Eq. (5), we then have:

$$(A - \nu B)\overline{\xi} = 0, \text{ with } \nu_i = \beta_i^2 \tag{14a}$$

$$\overline{\xi} = \{\overline{\xi}_{n,m}\}; B = \{B_{n,m}\}, B_{n,m} = \int_0^1 U(Y)\tilde{\Omega}_n(Y)\tilde{\Omega}_m(Y)dY \tag{14b-d}$$

$$A = \{A_{n,m}\}; \ A_{n,m} = \int_0^1 \tilde{\Omega}_m(Y)\frac{4}{\sigma^2}\frac{d}{dY}\left(K(Y)\frac{d\tilde{\Omega}_n(Y)}{dY}\right)dY =$$

$$= \frac{4}{\sigma^2}K(Y=1)\tilde{\Omega}_m(Y=1)\left.\frac{d\tilde{\Omega}_n(Y)}{dY}\right|_{Y=1} - \frac{4}{\sigma^2}\int_0^1 K(Y)\frac{d\tilde{\Omega}_m(Y)}{dY}\frac{d\tilde{\Omega}_n(Y)}{dY}dY \tag{14e,f}$$

whereas for the problem defined in Eq. (6) we have:

$$(A - \nu B)\overline{\zeta} = 0, \text{ with } \nu_i = \alpha_i^2 \tag{15a}$$

$$\overline{\zeta} = \{\overline{\zeta}_{n,m}\}; B = \{B_{n,m}\}, B_{n,m} = \int_0^1 U(Y)\tilde{\phi}_n(Y)\tilde{\phi}_m(Y)dY \tag{15b-d}$$

$$A = \{A_{n,m}\}; \ A_{n,m} = \int_0^1 \tilde{\phi}_m(Y)\frac{4}{\sigma^2}\frac{d}{dY}\left(K(Y)\frac{d\tilde{\phi}_n(Y)}{dY}\right)dY =$$

$$= -\frac{4}{\sigma^2}\int_0^1 K(Y)\frac{d\tilde{\phi}_m(Y)}{dY}\frac{d\tilde{\phi}_n(Y)}{dY}dY \tag{15e,f}$$

The algebraic problems, given by Eqs. (14) and (15), after truncation to a sufficiently large finite order M, are numerically solved, yielding results for the eigenvalues and eigenvectors. Then, the desired original eigenfunctions, $\xi_i(Y)$ and $\zeta_i(Y)$, can be readily constructed by recalling the inverse formulae given by Eqs. (11a) and (12a), respectively.

Then, operating on Eq. (1a) with $\int_0^1 \psi_i(Y,Z) - dY$ and making use of the boundary conditions along with Green's second identity, we obtain the following one-dimensional partial differential equations (PDE) system:

$$\frac{\partial\overline{\theta}_i(Z,\tau)}{\partial\tau} + \mu_i^2(Z)\overline{\theta}_i = g_i\left(Z,\tau,\overline{\boldsymbol{\theta}}\right), \quad i = 1,2,\dots \tag{16a}$$

where

$$g_i\left(Z,\tau,\overline{\boldsymbol{\theta}}\right) = -\sum_{j=1}^{\infty}\frac{\partial\overline{\theta}_j}{\partial Z}\int_0^1 W(Y)U(Y)\tilde{\psi}_i\tilde{\psi}_j dY$$

$$-\sum_{j=1}^{\infty}\frac{\partial^2\overline{\theta}_j}{\partial Z^2}\int_0^1\frac{K(Y)}{Pe^2}\tilde{\psi}_i\tilde{\psi}_j dY, \quad \overline{\boldsymbol{\theta}} = \left\{\overline{\theta}_1,\overline{\theta}_2,\dots\right\} \tag{16b,c}$$

with the transformed boundary and initial conditions given by:

$$\overline{\theta}_i(Z = -Z_{\text{ad},\infty},\tau) = \int_0^1 W(Y)\tilde{\psi}_i(Y)dY, \quad \left.\frac{\partial\overline{\theta}_i}{\partial Z}\right|_{Z=Z_\infty} = 0 \tag{16d,e}$$

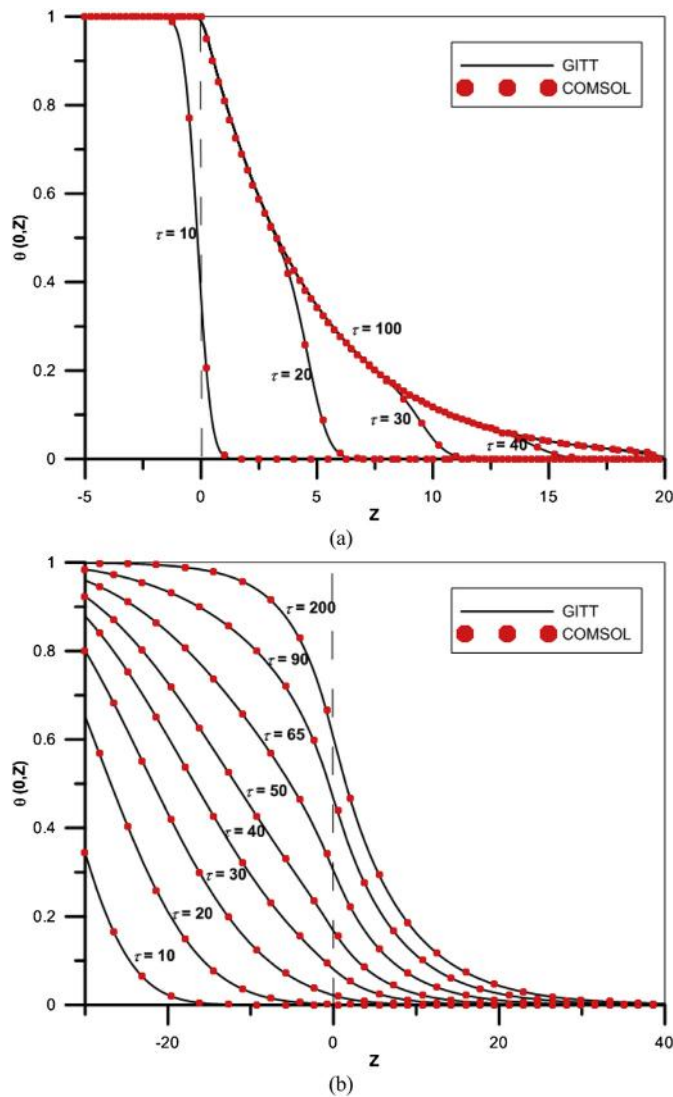$$\overline{\theta}_i(Z,\tau = 0) = 0 \tag{16f}$$

Fig. 2. Comparison between the dimensionless centerline temperature solution by means of the GITT with the single domain formulation and the purely numerical solution through COMSOL Multiphysics. (a)Pe = 27.476; (b)Pe = 0.5234.

Table 1(b)
Convergence behavior of the case with $Pe = 27.476$, with respect to the truncation order of the algebraic eigenvalue problem, M, with fixed $N = 10$.

| | $\tau = 20$ | | | |
M	$Z = 3$	$Z = 5$	$Z = 7$	$Z = 9$
$M = 20$	1.000	0.9902	0.6576	0.3761
$M = 30$	1.000	0.9894	0.6584	0.3777
$M = 40$	1.000	0.9892	0.6584	0.3776
$M = 50$	1.000	0.9894	0.6584	0.3775
$M = 60$	1.000	0.9893	0.6585	0.3776
	$\tau = 30$			
M	$Z = 3$	$Z = 5$	$Z = 9$	$Z = 13$
$M = 20$	1.000	0.9902	0.4282	0.1782
$M = 30$	1.000	0.9894	0.4287	0.1786
$M = 40$	1.000	0.9892	0.4288	0.1786
$M = 50$	1.000	0.9894	0.4288	0.1786
$M = 60$	1.000	0.9893	0.4288	0.1786

The PDE system given by Eq. (16), after truncated to a finite order N, sufficiently large to satisfy the accuracy needs, can be numerically solved to provide results for the transformed temperatures, $\bar{\theta}_i(Z, \tau)$. The *Mathematica* platform [44] provides the routine *NDSolve* for the solution of the PDE system here considered, under automatic absolute and relative errors control. Once the transformed potentials have been numerically computed, the *Mathematica* routine automatically provides an interpolation function object that approximates the Z and τ variables behavior of the solution in a continuous form. Then, the inversion formula (3b) can be recalled to yield the potential field representation θ at any desired position (Y,Z) and time τ.

3. Results and discussion

A numerical example is here considered as a rectangular microchannel with $L_f = 200$ μm height and $L_w = 40$ mm width, etched on a polyester resin substrate with $k_s = 0.16$ W/mK and $w_s = 1.482 \times 10^6$ J/m^3 K [41,43], and water as the working fluid ($k_f = 0.58$ W/mK and $w_f = 4.16 \times 10^6$ J/m^3 K). The microchannel external wall is assumed to be submitted to forced convection with air yielding Bi = 0.11($h_e = 60$ W/m^2 °C). A few test cases are considered by varying the thickness of the channel wall, L, which can be written in terms of the previously defined parameters as:

$$L = L_e - \frac{L_f}{2} \tag{17}$$

Table 1(a)
Convergence behavior of the case with $Pe = 27.476$, with respect to the truncation order of the temperature field expansion, N, with fixed $M = 60$.

| | $\tau = 20$ | | | |
N	$Z = 3$	$Z = 5$	$Z = 7$	$Z = 9$
$N = 2$	1.000	0.9892	0.6582	0.3772
$N = 4$	1.000	0.9892	0.6585	0.3776
$N = 6$	1.000	0.9892	0.6584	0.3775
$N = 8$	1.000	0.9892	0.6585	0.3775
$N = 10$	1.000	0.9893	0.6585	0.3776
COMSOL	1.000	0.9998	0.6524	0.3731
	$\tau = 30$			
N	$Z = 3$	$Z = 5$	$Z = 9$	$Z = 13$
$N = 2$	1.000	0.9892	0.4286	0.1785
$N = 4$	1.000	0.9892	0.4288	0.1786
$N = 6$	1.000	0.9892	0.4288	0.1786
$N = 8$	1.000	0.9892	0.4288	0.1786
$N = 10$	1.000	0.9893	0.4288	0.1786
COMSOL	1.000	0.9998	0.4249	0.1768

Table 2(a)
Convergence behavior of the case with $Pe = 0.5234$, with respect to the truncation order of temperature field expansion, N, with fixed $M = 60$.

| | $\tau = 50$ | | | |
N	$Z = -20$	$Z = -10$	$Z = 0$	$Z = 10$
$N = 2$	0.7278	0.4474	0.1666	0.02522
$N = 4$	0.7278	0.4474	0.1666	0.02523
$N = 6$	0.7278	0.4474	0.1666	0.02523
$N = 8$	0.7278	0.4474	0.1666	0.02523
$N = 10$	0.7278	0.4474	0.1666	0.02523
COMSOL	0.7277	0.4474	0.1696	0.02559
	$\tau = 90$			
N	$Z = -20$	$Z = -10$	$Z = 0$	$Z = 10$
$N = 2$	0.9344	0.8132	0.4645	0.1119
$N = 4$	0.9344	0.8132	0.4645	0.1119
$N = 6$	0.9344	0.8132	0.4645	0.1119
$N = 8$	0.9344	0.8132	0.4645	0.1119
$N = 10$	0.9344	0.8132	0.4645	0.1119
COMSOL	0.9343	0.8137	0.4705	0.1129

Table 2(b)
Convergence behavior of the case with $Pe = 0.5234$, with respect to the truncation order of the algebraic eigenvalue problem, M, with fixed $N = 10$.

| | $\tau = 50$ | | | |
M	$Z = -20$	$Z = -10$	$Z = 0$	$Z = 10$
$M = 20$	0.7278	0.4475	0.1702	0.02574
$M = 30$	0.7278	0.4474	0.1667	0.02525
$M = 40$	0.7278	0.4474	0.1666	0.02523
$M = 50$	0.7278	0.4474	0.1667	0.02525
$M = 60$	0.7278	0.4474	0.1666	0.02523
	$\tau = 90$			
M	$Z = -20$	$Z = -10$	$Z = 0$	$Z = 10$
$M = 20$	0.9345	0.8139	0.4725	0.1136
$M = 30$	0.9344	0.8133	0.4649	0.1120
$M = 40$	0.9344	0.8132	0.4646	0.1119
$M = 50$	0.9344	0.8133	0.4649	0.1120
$M = 60$	0.9344	0.8132	0.4646	0.1119

Before proceeding to the discussion of the selected cases, a verification is performed on the solution methodology herein proposed by comparing the results against purely numerical solutions obtained through the commercial solver COMSOL Multiphysics, based on the finite element method. For this verification, the channel thickness $L = 100$ μm and two different volumetric flow rates, 5.04 mL/min and 0.096 mL/min, have been selected, yielding two very different Péclet numbers, $Pe = 27.476$ and $Pe = 0.5234$, respectively. Fig. 2 (a,b) show the fluid temperature at the channel centerline along the channel length for these two cases, respectively, presenting both the GITT solution with the single domain approach, and the COMSOL Multiphysics solution. One may observe that for both cases, despite such very distinct behavior due to the differences in Péclet numbers, the GITT and COMSOL solutions are essentially coincident for all selected times. Regarding the physics of the problem, it may be observed in Fig. 2(a) that with $Pe = 27.476$ the influence of the upstream region is significant only at the early time stages, whereas in Fig. 2(b), with $Pe = 0.5234$, the influence of the upstream region is clearly observed.

In order to provide further discussions on the GITT solution with the single domain approach, the convergence behavior of the solution for the case with $Pe = 27.476$ is presented in Table 1(a,b). First, Table 1(a) shows the converge behavior of the eigenfunction expansion by varying the truncation order N in the expansion in Eq. (3b), with fixed $M = 60$ terms in the truncation of the algebraic eigenvalue problems defined in Eqs. (14) and (15), for two different times, $\tau = 20$ and $\tau = 30$, presenting full convergence to at least four significant digits. The COMSOL solution is also presented, being in agreement with the GITT solution in at least two significant digits. Table 1(b) shows the convergence behavior of the solution concerning the truncation order M employed in the algebraic eigenvalue problems in Eqs. (14) and (15), keeping the truncation order N in the expansion in Eq. (3b) fixed with $N = 10$ terms, and showing a consistent convergence behavior of at least three significant digits. Similar results are illustrated in Table 2(a,b) for the case with $Pe = 0.5234$, where an overall convergence of at least three significant digits is observed. The COMSOL results are also illustrated, presenting an agreement of three significant digits in almost all selected positions and times.

Table 3
Channel wall thickness of the test cases and calculated dimensionless parameters.

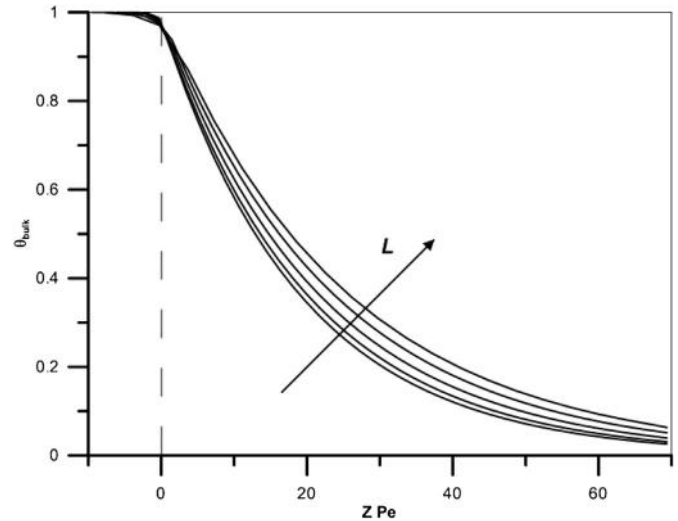| Case	Wall thickness, L	Bi, Eq. (2)	σ, Eq. (2)
1	$L = 900$ μm	Bi $= 0.375$	$\sigma = 5$
2	$L = 650$ μm	Bi $= 0.28125$	$\sigma = 3.75$
3	$L = 400$ μm	Bi $= 0.1875$	$\sigma = 2.5$
4	$L = 200$ μm	Bi $= 0.1125$	$\sigma = 1.5$
5	$L = 75$ μm	Bi $= 0.06562$	$\sigma = 0.875$

Fig. 3. Dimensionless fluid bulk temperature along the channel length for five different channel wall thicknesses ($L = 900, 650, 400, 200, 75$ μm) − steady state.

Now we proceed to the investigation of the selected test cases with different channel wall thicknesses and considering a volumetric flow rate of 0.5 mL/min, yielding $Pe = 3$. Table 3 shows the five channel wall thicknesses considered and the corresponding calculated dimensionless parameters, Bi and σ, in Eq. (2).

Fig. 3 illustrates the dimensionless bulk temperature distribution along the channel length at steady-state, for the five thicknesses presented in Table 3. It can be observed that decreasing the thickness leads to an expected more effective cooling along the channel, as consequence of less thermal resistance across the transversal direction. From the mathematical point of view, one may observe that decreasing the thickness implies in increasing the term $4/\sigma^2$, which affects the transversal diffusion term. It is also observed that the pre-cooling that takes place at the upstream region is slightly more effective when the thickness is increased, which is explained by the increased relative relevance of the axial conduction term with respect to the transversal diffusion term for increasing thickness, and becomes less significant when the channel wall thickness is decreased.
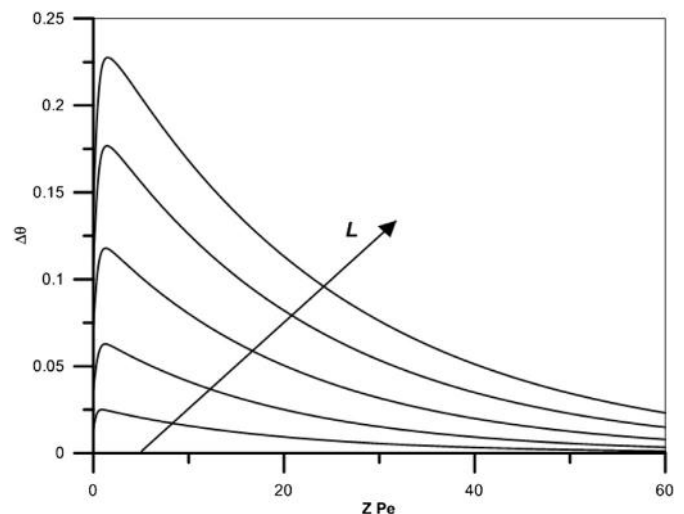

Fig. 4. Difference between the dimensionless internal and external wall temperatures along the channel length for five different wall thicknesses, at steady state ($L = 900, 650, 400, 200, 75$ μm).
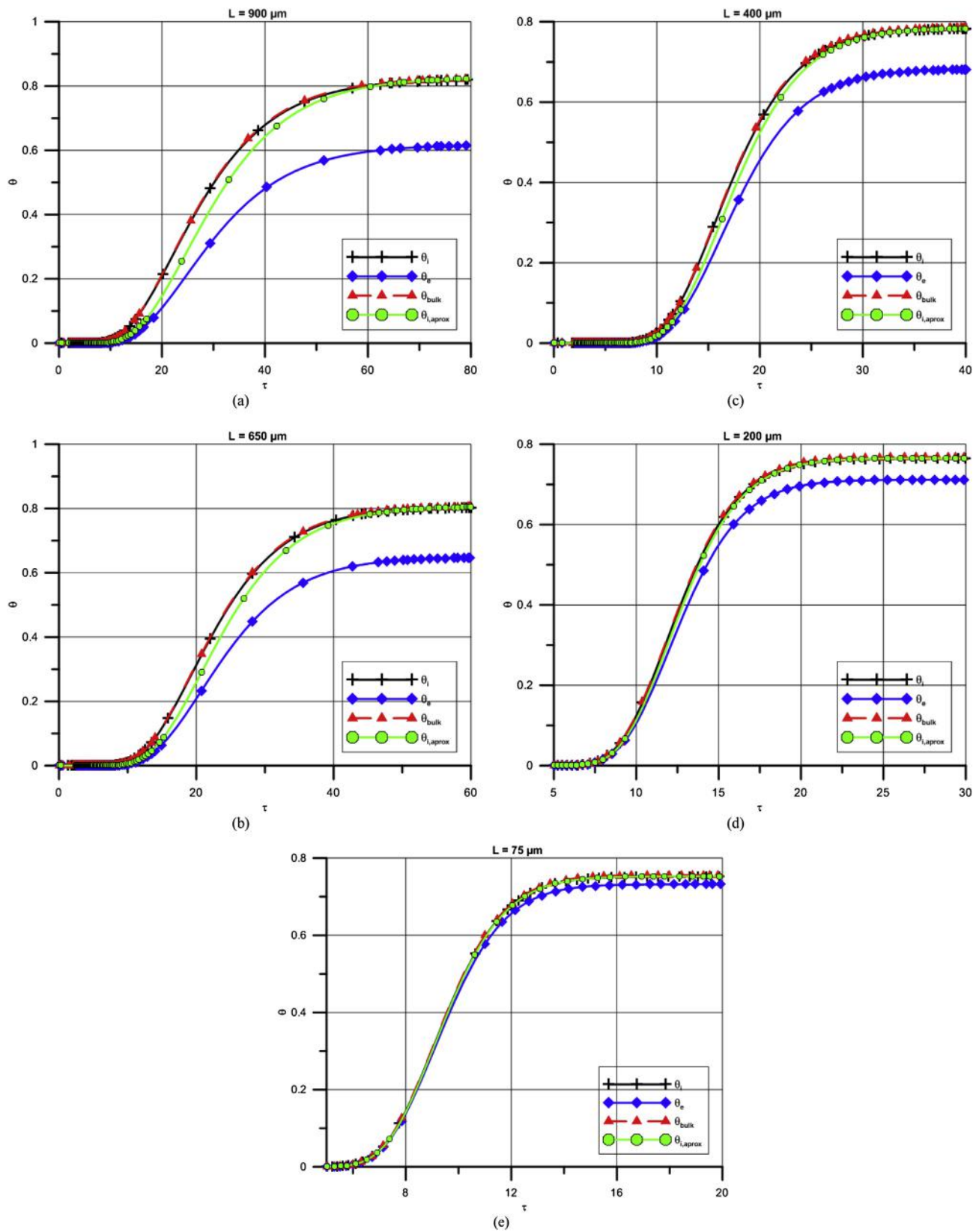
Fig. 5. Time evolution of the dimensionless internal wall temperature, external wall temperature, fluid bulk temperature and the approximate internal wall temperature obtained from Eq. (11), at ZPe = 5, for different wall thicknesses (a) $L = 900$ μm, (b) $L = 650$ μm, (c) $L = 400$ μm, (d) $L = 200$ μm and (e) $L = 75$ μm.
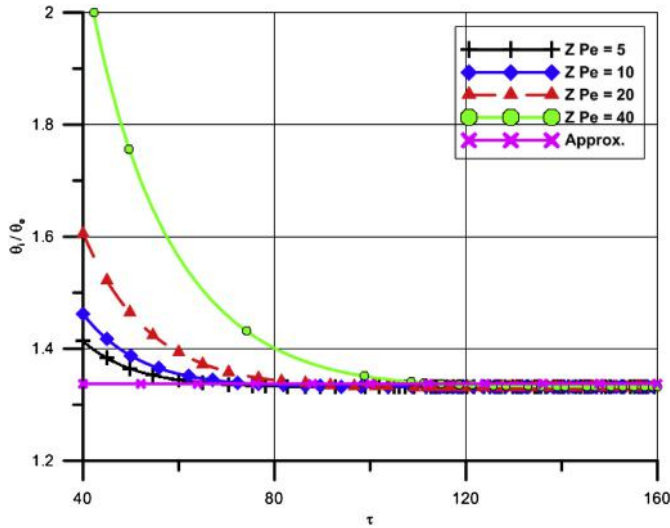
Fig. 6. Ratios between the dimensionless temperature at the internal face of the channel and the temperature at the external face of the channel, along the transient state for different longitudinal positions, in comparison with the approximation of Eq. (18). Case 1: $L = 900$ μm.

Fig. 7. Time evolution of the external wall temperature at ZPe $= 5$ for five wall thicknesses ($L = 900, 650, 400, 200,$ and 75 μm).

The influence of the thermal resistance due to the channel wall is better observed in Fig. 4, that presents the difference between the dimensionless temperature at the external wall (the interface with the surrounding environment) and the temperature at the internal wall (the interface with the fluid stream) along the channel length, at steady state. One may observe that the temperature difference is significantly higher at the region in the vicinity of the entrance of the heat exchange section and then decreases along the channel length. It is interesting to note that the temperature difference at the entrance of the heat exchange section is not the highest, because of the transition from the insulated upstream region, which presents small transversal temperature gradients.

One important aspect involving conjugated heat transfer in microchannels is how accurately the temperatures at the internal wall can be inferred from temperature measurements at the external wall, which can be directly obtained, for instance, by means of an infrared thermography system with microscopic lenses [41]. Assuming that all the energy that is dissipated at the external wall to the surrounding environment arrives from transversal diffusion and neglecting the heat capacitance of the channel wall, we have the following approximate relation for the dimensionless internal and external wall temperatures, based upon a simple thermal resistance model:

$$\theta_{i,\text{aprox}}(Z, \tau) = Bi \frac{L}{L_e} \theta(Y = 1, Z, \tau) \qquad (18)$$

Fig. 5 show the time evolutions of the dimensionless fluid bulk temperature, the dimensionless temperatures of the external and internal walls and the approximate dimensionless temperature of the internal wall as calculated from Eq. (18). The axial position has been intentionally chosen at ZPe $= 5$, which is a position where high temperature differences are observed (Fig. 3). The five cases presented in Table 3 are shown here, namely: (a) $L = 900$ μm, (b) $L = 650$ μm, (c) $L = 400$ μm, (d) $L = 200$ μm and (e) $L = 75$ μm. For the case of the thickest channel wall, in Fig. 5(a), we observe that the approximate temperatures at the internal wall achieve a fairly good agreement with the actual internal temperatures at steady state, but along the transient the approximations are not so good, offering lower predictions than the temperatures calculated through the full conjugated model. This deviation is explained
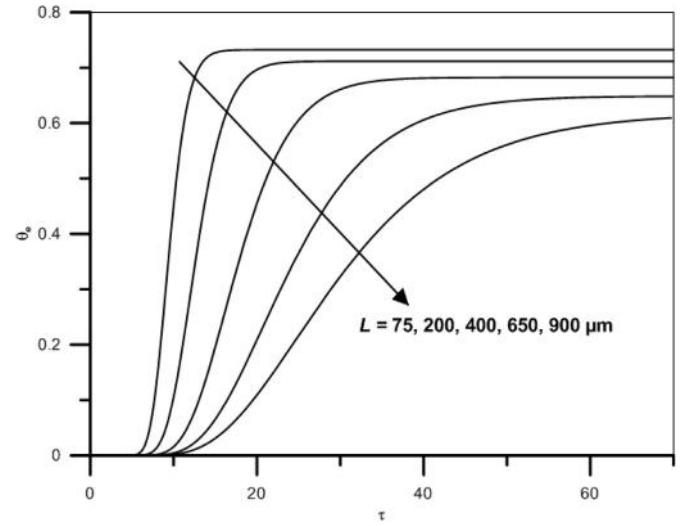
mainly by the thermal capacitance of the wall, which may not be neglected in this case. For $L = 200$ μm and smaller thicknesses, reasonable estimates of the internal wall temperatures are still obtained with Eq. (18), even during the transient, since the effects of the wall thermal capacitance are not so significant. Another interesting aspect observed in Fig. 5 is that the fluid bulk temperature is not so different from the internal wall temperature, in light of the large heat transfer coefficients that can be achieved. Thus, in such examples, good approximations of the fluid bulk temperature can be inferred from temperature measurements at the external wall of the channel with the use of Eq. (18), especially at steady state. In order to illustrate the approximation behavior during the transient state at other axial positions, Fig. 6 shows the ratios between the temperature at the internal face of the channel and the temperature at the external face of the channel for four different axial positions: Z Pe $= 5$, 10, 20 and 40, in the case with $L = 900$ μm. The ratio provided by the approximation in Eq. (18) is also shown, which is constant due to the neglect of the thermal capacitance. One may observe that for positions farer from the entrance, the
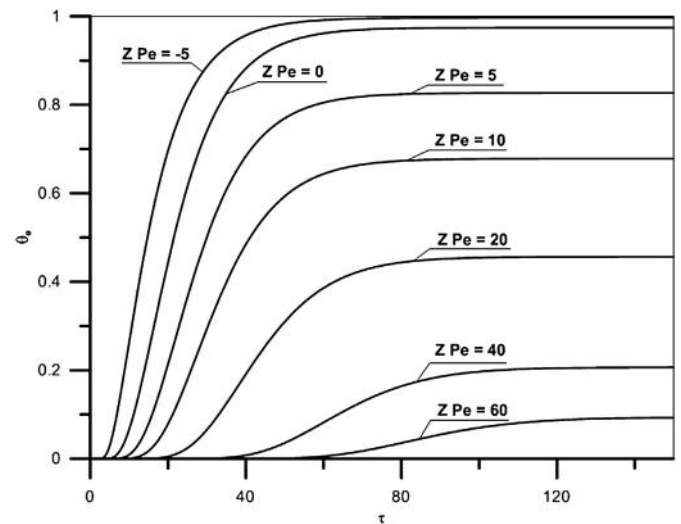

Fig. 8. Time evolution of the external wall temperature for different axial positions – Case 1: $L = 900$ μm.

ratio computed from the full conjugated model takes more time to reach the asymptotic behavior, as result of the increased time needed to reach steady state at those positions, as it will be discussed later. Nonetheless, in all cases the asymptotic behaviors of the ratio provided by the temperatures from the full conjugated model are fairly close to the approximate temperature ratio value.

Fig. 7 brings a comparison of the transient behaviors of the dimensionless external wall temperature at ZPe = 5 for the five test cases here considered. These results show that the thickness of the channel wall significantly affects the time needed for the establishment of the steady state, which becomes significantly higher for increasing thickness. Finally, Fig. 8 shows the transient behavior of the external wall temperature of Case 1 ($L = 900$ μm) for different axial positions. It can be observed that the positions farer from the entrance require significantly more time for the establishment of the steady state, being needed up to $\tau = 150$ for the whole channel length to reach steady state in the present illustration, which corresponds to more than 170 s for the considered dimensional parameters, much higher than in principle expected for a microchannel convective heat transfer situation without wall conjugation.

4. Conclusions

Internal transient forced convection with full channel walls participation is here analyzed, with particular emphasis on liquid flow micro-scale applications. A recently developed methodology for the analysis of conjugated convective-conductive heat transfer problems, consisting of a single-domain formulation combined with the generalized integral transform technique (GITT), is here further advanced in order to tackle transient conjugated problems, taking into account both transversal and axial diffusion effects, and including pre-heating or pre-cooling of the region upstream of the heat exchange section. An existing experimental configuration is considered, consisting of a rectangular microchannel etched on a polyester resin substrate, with different wall thicknesses. This test case is also used to verify the accuracy and merits of a simple thermal resistance model across the wall thickness in estimating the internal wall temperature from available measurements of the external wall temperatures. The results obtained with the methodology herein proposed with user-prescribed accuracy were directly compared to purely numerical solutions obtained through the commercial CFD simulation tool COMSOL Multiphsyics, presenting excellent agreement.

Acknowledgements

References

[1] S. Kakaç, Y. Yener, Exact solution of the transient forced convection energy equation for timewise variation of inlet temperature, Int. J. Heat Mass Transf. 16 (1973) 2205–2214.

[2] S. Kakaç, A general solution to the equation of transient forced convection with fully developed flow, Int. J. Heat Mass Transf. 18 (1975) 449–1453.

[3] S. Kakaç, Y. Yener, Transient laminar forced convection in ducts, in: S. Kakaç, R.K. Shah, A.E. Bergles (Eds.), Low Reynolds Number Flow Heat Exchangers, 1983, pp. 205–227. Hemisphere, New York.

[4] R.M. Cotta, M.N. Ozisik, Transient forced convection in laminar channel flow with stepwise variations of wall temperature, Can. J. Chem. Eng. 64 (1986) 734–742.

[5] R.M. Cotta, M.N. Ozisik, D.S. McRae, Transient heat transfer in channel flow with step change in inlet temperature, Numer. Heat Transf. 9 (1986) 619–630.

[6] R.M. Cotta, M.N. Ozisik, Laminar forced convection in ducts with periodic variation of inlet temperature, Int. J. Heat Mass Transf. 29 (10) (1986) 1495–1501.

[7] R.M. Cotta, M.D. Mikhailov, M.N. Ozisik, Transient conjugated forced convection in ducts with periodically varying inlet temperature, Int. J. Heat Mass Transf. 30 (10) (1987) 2073–2082.

[8] S. Kakaç, W. Li, R.M. Cotta, Unsteady laminar forced convection in ducts with periodic variation of inlet temperature, J. Heat Transf. 112 (1990) 913–920.

[9] S. Kakaç, R.M. Cotta, Experimental and theoretical investigation on transient cooling of electronic systems, in: Proc.. of the NATO Advanced Study Institute on Cooling of Electronic Systems, Invited Lecture, NATO ASI Series E: Applied Sciences, vol. 258, June/July, 1993, pp. 239–275. Turkey.

[10] R.M. Cotta, J.E.V. Gerk, Mixed finite difference/integral transform approach for parabolic-hyperbolic problems in transient forced convection, Numer. Heat Transf. B Fundam. 25 (1994) 433–448.

[11] C.A.C. Santos, D.M. Brown, S. Kakaç, R.M. Cotta, Analysis of unsteady forced convection in turbulent duct flow, J. Thermophys. Heat Transf. 9 (3) (1995) 508–515.

[12] R.M. Cotta, Integral transforms in transient convection: benchmarks and engineering simulations, in: Invited Keynote Lecture, ICHMT International Symposium on Transient Convective Heat Transfer, Turkey, August, 1996, pp. 433–453.

[13] C.A.C. Santos, M.J. Medeiros, R.M. Cotta, S. Kakaç, Theoretical analysis of transient laminar forced convection in simultaneous developing flow in parallel-plate channel, in: 7th AIAA/ASME Joint Themophysics and Heat Transfer Conference, AIAA Paper #97–2678, June, 1998. Albuquerque, New Mexico.

[14] S. Cheroto, M.D. Mikhailov, S. Kakaç, R.M. Cotta, Periodic laminar forced convection: solution via symbolic computation and integral transforms, Int. J. Therm. Sci. 38 (7) (1999) 613–621.

[15] S. Kakaç, C.A.C. Santos, M.R. Avelino, R.M. Cotta, Computational solutions and experimental analysis of transient forced convection in ducts, invited paper, Int. J. Transp. Phenom. 3 (2001) 1–17.

[16] R.M. Cotta, H.R.B. Orlande, M.D. Mikhailov, S. Kakaç, Experimental and theoretical analysis of transient convective heat and mass transfer: hybrid approaches, in: Invited Keynote Lecture, ICHMT International Symposium on Transient Convective Heat and Mass Transfer in Single and Two-Phase Flows, Cesme, Turkey, August 17–22, 2003.

[17] G. Tunc, Y. Bayazitoglu, Convection at the entrance of micropipes with sudden wall temperature change, in: ASME 2002 International Mechanical Engineering Congress and Exposition Heat Transfer, vol. 1, November 17–22, 2002. New Orleans, Louisiana, USA.

[18] R.M. Cotta, S. Kakaç, M.D. Mikhailov, F.V. Castellões, C.R. Cardoso, Transient flow and thermal analysis in microfluidics, in: S. Kakaç, L.L. Vasiliev, Y. Bayazitoglu, Y. Yener (Eds.), Microscale Heat Transfer — Fundamentals and Applications, NATO ASI Series, Kluwer Academic Publishers, The Netherlands, 2005, pp. 175–196.

[19] F.V. Castellões, R.M. Cotta, Analysis of transient and periodic convection in microchannels via integral transforms, Prog. Comput. Fluid Dyn. 6 (6) (2006) 321–326.

[20] F.V. Castellões, C.R. Cardoso, P. Couto, R.M. Cotta, Transient analysis of slip flow and heat transfer in microchannels, Heat Transf. Eng. 28 (6) (2007) 549–558.

[21] R.M. Cotta, C.A.A. Mota, C.P. Naveira-Cotta, J.S. Nunes, M.R. Avelino, F.V. Castellões, J.N.N. Quaresma, Heat transfer enhancement in laminar forced convection: nanofluids, microchannels, structured surfaces, in: Invited Keynote Lecture, ICCHMT International Symposium on Convective Heat and Mass Transfer in Sustainable Energy, CONV-09, April, 2009, p. 38. Yasmine Hammamet, Tunisia. http://dx.doi.org/10.1615/ICHMT.2009.CONV.60.

[22] F.V. Castellões, J.N.N. Quaresma, R.M. Cotta, Convective heat transfer enhancement in low Reynolds number flows with wavy walls, Int. J. Heat Mass Transf. 53 (2010) 2022–2034.

[23] R.M. Cotta, Hybrid numerical-analytical approach to nonlinear diffusion problems, Numer. Heat Transf. B Fundam. 127 (1990) 217–226.

[24] R.M. Cotta, Integral Transforms in Computational Heat and Fluid Flow, CRC Press, Boca Raton, FL, 1993.

[25] R.M. Cotta, Benchmark results in computational heat and fluid flow: the integral transform method, Int. J. Heat Mass Transf. 37 (Suppl. 1) (1994) 381–394 (Invited Paper).

[26] R.M. Cotta, M.D. Mikhailov, Heat Conduction: Lumped Analysis, Integral Transforms, Symbolic Computation, Wiley-Interscience, Chichester, UK, 1997.

[27] R.M. Cotta, The Integral Transform Method in Thermal and Fluids Sciences and Engineering, Begell House, New York, 1998, p. 430.

[28] R.M. Cotta, M.D. Mikhailov, Hybrid methods and symbolic computations, in: W.J. Minkowycz, E.M. Sparrow, J.Y. Murthy (Eds.), Handbook of Numerical Heat Transfer, second ed., Wiley, New York, 2006 (Chapter 16).

[29] T.F. Lin, J.C. Kuo, Transient conjugated heat transfer in fully developed laminar pipe flows, Int. J. Heat Mass Transf. 31 (5) (1988) 1093–1102.

[30] S. Olek, E. Elias, E. Wacholder, S. Kaizerman, Unsteady conjugated heat transfer in laminar pipe flow, Int. J. Heat Mass Transf. 34 (6) (1991) 1443–1450.

[31] R.O.C. Guedes, R.M. Cotta, Periodic laminar forced convection within ducts including wall heat conduction effects, Int. J. Eng. Sci. 29 (5) (1991) 535—547.

[32] W.-M. Yan, Transient conjugated heat transfer in channel flows with convection from the ambient, Int. J. Heat Mass Transf. 36 (5) (1993) 1295—1301.

[33] R.O.C. Guedes, M.N. Ozisik, R.M. Cotta, Conjugated periodic turbulent forced convection in a parallel plate channel, J. Heat Transf. 116 (1994) 40—46.

[34] S. Bilir, A. Ates, Transient conjugated heat transfer in thick walled pipes with convective boundary conditions, Int. J. Heat Mass Transf. 46 (2003) 2701—2709.

[35] C.P. Naveira, M. Lachi, R.M. Cotta, J. Padet, Hybrid formulation and solution for transient conjugated conduction-external convection, Int. J. Heat Mass Transf. 52 (1—2) (2009) 112—123.

[36] J.S. Nunes, R.M. Cotta, M. Avelino, S. Kakaç, Conjugated heat transfer in microchannels, in: S. Kakaç, B. Kosoy, A. Pramuanjaroenkij (Eds.), Microfluidics Based Microsystems: Fundamentals and Applications, NATO Science for Peace and Security Series A: Chemistry and Biology, vol. 1, 2010, pp. 61—82. Org.

[37] R.O.C. Guedes, R.M. Cotta, N.C.L. Brum, Heat transfer in laminar tube flow with wall axial conduction effects, J. Thermophys. Heat Transf. 5 (4) (1991) 508—513.

[38] D.C. Knupp, C.P. Naveira-Cotta, R.M. Cotta, Theoretical analysis of conjugated heat transfer with a single domain formulation and integral transforms, Int. Commun. Heat Mass Transf. 39 (3) (2012) 355—362.

[39] D.C. Knupp, C.P. Naveira-Cotta, R.M. Cotta, Conjugated convection-conduction analysis in microchannels with axial diffusion effects and a single domain formulation, ASME J. Heat Transf. 135 (9) (2013) 091401.

[40] D.C. Knupp, R.M. Cotta, C.P. Naveira-Cotta, Conjugated heat transfer in microchannels with upstream-downstream regions coupling, Numer. Heat Transf. B Fundam. 64 (5) (2013) 365—387.

[41] D.C. Knupp, R.M. Cotta, C.P. Naveira-Cotta, Conjugated heat transfer in heat spreaders with micro-channels, in: Proc. of the ASME 2013 Summer Heat Transfer Conference, HT2013, Minneapolis, MN, USA, July 14—19, 2013.

[42] C.P. Naveira-Cotta, R.M. Cotta, H.R.B. Orlande, O. Fudym, Eigenfunction expansions for transient diffusion in heterogeneous media, Int. J. Heat Mass Transf. 52 (2009) 5029—5039.

[43] D.C. Knupp, C.P. Naveira-Cotta, J.V.C. Ayres, R.M. Cotta, H.R.B. Orlande, Theoretical-experimental analysis of heat transfer in non-homogeneous solids via improved lumped formulation, integral transforms and infrared thermography, Int. J. Therm. Sci. 62 (2012) 71—84.

[44] S. Wolfram, The Mathematica Book, Wolfram Media, Cambridge, 2005.